Proceeding of the 7th International Symposium on Artificial Intelligence, Robotics and Automation in Space: i-SAIRAS 2003, NARA, Japan, May 19-23, 2003

Improving the Free-floater Space Robot Simulator for Intervention Missions

C. Bettanini, A. Aboudan, A. Francesconi, M. Marchesi, C. Menon, G. Bianchini and F.Angrilli
"G. Colombo" Center of Studies and Activities for Space - CISAS
Department of Mechanical Engineering - University of Padova
via Venezia, 1, 35131 Padova , Italy
carlo.bettanini@unipd.it

Keywords
Space robotics, free-flyer robot, on orbit servicing, microgravity simulator, non-holonomic constraint, manipulation, object capture, Extra Vehicular Activity.

Abstract
The increasing application of robots in hazardous space environments and in support of extra vehicular activities has drawn attention to problems related with robust and safe application of free flyer space robots. As a key point in addressing these topics CISAS has since 1996 worked on the development and construction of free floating robots to be used in laboratory tests under micro gravity conditions.
The free floater robot architecture is composed by two main parts: the floating base, that is free to move and rotate on a plane, and an anthropomorphic manipulator with three degrees of freedom, connected to the base.
The two dimensional micro gravity condition is achieved by means of low pressure air bearings, that are located under the robot and allow it to float over a low roughness, high planarity granite table. Friction reduction is so effective that residual disturbing accelerations in the order of 10^{-5} g have been measured. Control of the capture operation is possible through the elaboration of object location and configuration from a visual system (CCD camera, frame grabber and elaboration software) and manipulator sensors (encoders). An extensive campaign of tests has been conducted in order to prove the ability of the robot to grab with the manipulator a free floating object passing over the plane starting from a random position. To improve the already satisfying results of the first prototypes of the free floater robot, a set of actions has been promoted. Last technological developments are related to increase overall efficiency through components improvement, speed up elaboration time and reduce overall weight thus increasing zero gravity autonomy.
The ongoing optimisation activity is related to the following new aspects : CPU calculation through a PC 104 plus axes control board, resulting in a position measurement and estimator with higher frequency rate, multi-tasking real time software on board for faster data acquisition, elaboration and command processing.
Also, one of the main drawbacks of the former configuration, concerning the use of Led on both robot arm and target, will be mitigated by means of last generation frame grabber in conjunction with higher definition cameras.
In the future a second camera will be installed on board in parallel with an on board PC 104 frame grabber in order to address vision problems related to on board tracking of moving targets, estimation of tumbling trajectories, docking and rendezvous optimisation in the robot fixed frame.
CISAS is also working on extension of the 2D robot technologies to a three dimensional testbed dedicated to parabolic flight tests. This will allow to optimise base control strategies without thruster firings for a free flying 3D robot with comparable mass and inertia of base and arm.

1. Introduction

Robotics is to date playing a key role in scientific and commercial space missions, performing hazardous and heavy duty tasks as well as high precision operations. Reliability and affordability of robotic technologies will in the future be one of the main drivers for space exploitation in the light of foreseeable space scenarios, that involve orbital assembly of large structures and servicing of orbital systems. Space industry and as well governmental agencies have been in the last years recognising the potentials offered by robot assisted on-orbit servicing to change the economy of space and this has driven to the definition of servicing demonstration missions as the planned Orbital Express system by DARPA, XEUS and TECSAS projects by European space agencies and the Robonaut project by NASA. All these missions rely deeply on autonomous robotic technologies, that cope with the control of the complex dynamic behaviour of robotic free flyer systems. In this field great interest has driven the possibility to minimise the dynamic coupling between arm and base motion and to consequently reduce required corrections performed by attitude control system, which drive to fuel depletion impacting on mission costs and lifetime.

Therefore work is carried on both on autonomous 2D free floaters and on a 3D thrustless free flyer demonstrator in order to investigate and optimise simply coded control strategies that allow target capture with minimal impact on base motion.

2 Free Floater Robot & Test bed Upgrading

The experimental test bed, which architecture is shown in figure 2.1, allows to perform simulations of autonomous tracking and capture operations with robot and target floating over a low roughness, high planarity granite table by means of low pressure air bearings. Robot is composed by an anthropomorphic manipulator with three degrees of freedom connected to the floating base, equipped with eight air thrusters to control trajectory and base attitude.

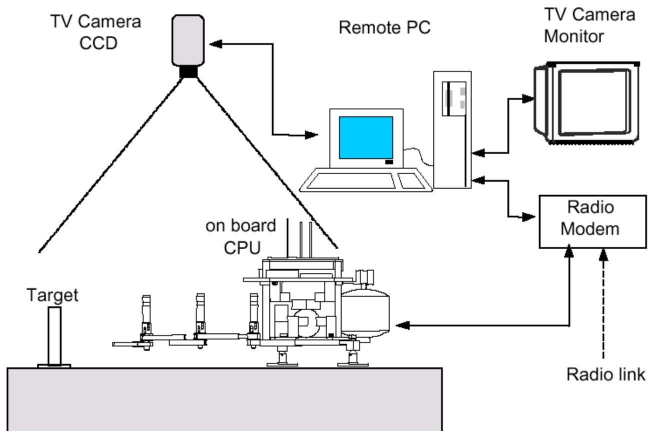

Fig. 2.1:Experimental test bed for floating robot

An extensive test campaign has been conducted in last years and results have been presented in [1]. Test bed is to date undergoing an extensive upgrade in order to increase overall system efficiency trough mechanical and electronic components improvement.
The ongoing optimisation activity is related to the following new aspects:

- ✓ Mechanical and electronic optimisation of the robot, which will drive to faster elaboration time and to overall weight reduction allowing to speed up navigation loop and increase zero g autonomy.
- ✓ Vision System upgrading, thanks to a new vision system and improved vision algorithm which will allow to measure position and attitude of free floating robot without the need of led on several base position.
- ✓ A propulsion system arrangement of innovative design, which gives the possibility to regulate thrust intensity by utilising original prototype on /off electron-valves in series with a small reservoir obtaining an effect similar to that of a variable-section thruster.

2.1 Upgrade of Mechanics and Electronics

On going optimisation benefits from latest technological developments mainly in electronic components miniaturisation. The former robot configuration , shown in figure 2.2, had the following overall dimensions: 855 x 456 x 451 and a weight of 27 kg.

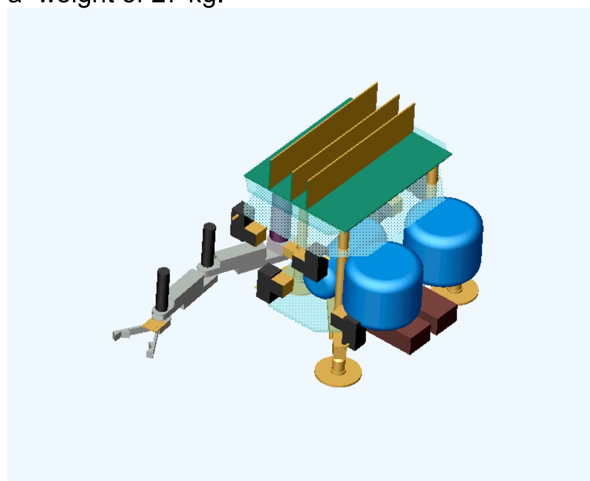

Fig. 2.2: Former 2D Autonomous Robot configuration

The improved robot architecture is characterised by the following new aspects:
CPU calculation is performed by a fast PC 104 main board and axes control is carried out by a dedicated PC 104 board, resulting in a position measurement and estimation with higher frequency rate and almost halved housing dimension requirements .
A new frame, obtained with light weight materials has been engineered, achieving components layout optimisation and increased standardisation and maintainability of the system. The new design implies the following overall dimensions: 855 x 356 x 251 and an estimated reduced weight of 16 kg.
Software elaboration relies on a new multi-tasking real time software on QNX operative system running on PC 104 for faster data acquisition, elaboration and command processing.
Image elaboration is to date performed by a remote PC but an on board camera with the relative PC 104 frame grabber has already been tested in software architecture and will be installed for on board tracking simulation .

2.2 Upgrade of Vision System

Capture operations require the measurement of robot and target position and attitude whit respect to an inertial reference frame at a rate of 20 Hz. This task is performed using a vision-based tracking system. The set-up of vision system consists of:

1. CCD camera
2. Frame grabber PCI interface card.
3. PC.
4. C++ code to process image data.

A calibration phase is performed for estimate the intrinsic and extrinsic parameters of the CCD camera whit respect to the inertial frame.

The vision algorithm performs three main steps: first the corners of objects in the scene are extracted. A geometric model of the robot and of the target is used to segment the scene and track their rigid motion, afterward a pose estimation algorithm uses the selected features to obtain the desired measurements.

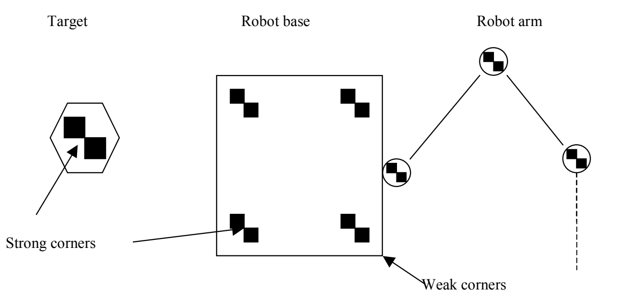

Fig. 2.3 – Sketch of vision system marker disposition

Defining q_R the joint variables of robot, q_B the joint variable of the moving base, q_A the joint variables of the arm and q_T the position of target:

$$q_R := \begin{bmatrix} q_B \\ q_A \end{bmatrix} \quad , \quad q_B := \begin{bmatrix} x_B \\ y_B \\ \theta_B \end{bmatrix} \quad , \quad q_A := \begin{bmatrix} \theta_1 \\ \vdots \\ \theta_N \end{bmatrix} \quad , \quad q_T := \begin{bmatrix} x_T \\ y_T \end{bmatrix}$$

Strong features are attached on the target, the robot and its arm; this features can be easily extracted from the image using a Sobel filter corner detector.

The segmentation section of algorithm assigns at each corner the probability of coming from the target, the robot base, the robot arm or the background using the a-priori knowledge of geometry and dynamics of these moving objects. The corners assigned at background are discarded.

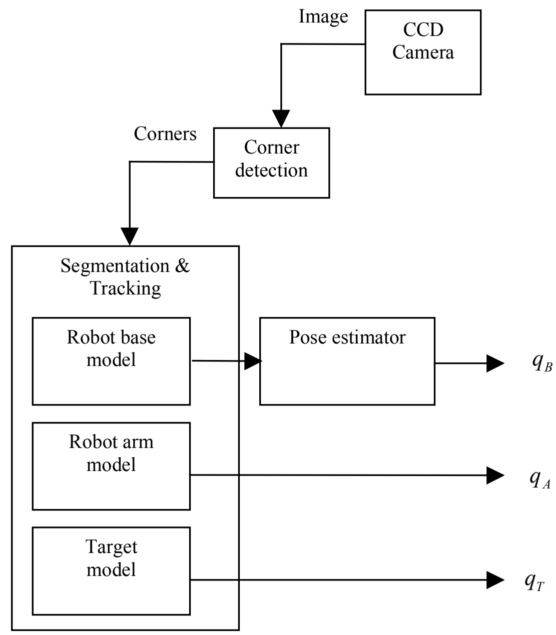

Fig. 2.4 – Scheme of Tracking Algorithm

Supposing that the corners extracted from image at time t-1 , Y(t-1) , are divided by the algorithm into Y_A(t-1), Y_b(t-1), and Y_T(t-1) (respectively the corners from the arm, the base and the target) the story of observations relative to the base , arm and target position can be the following:

$$Y_A(t-1) := \{y_A(0), \ldots, y_A(t-1)\}$$
$$Y_B(t-1) := \{y_B(0), \ldots, y_B(t-1)\}$$
$$Y_T(t-1) := \{y_T(0), \ldots, y_T(t-1)\}$$

The known geometry of the objects, the cinematic of the free floating robots and a model of the (calibrated) pinhole camera allows to define the observation probabilities as

$$p(y_A(t) | q_A(t)) \, , \, p(y_B(t) | q_B(t)) \, , \, p(y_T(t) | q_T(t))$$

The dynamics of the objects, the velocities $\dot{q}_A(t-1)$, $\dot{q}_B(t-1)$, $\dot{q}_T(t-1)$ and the command $\tau(t-1)$ computed from the controller of the robot are used to perform the propagation of conditional probability density of joint variables [2].

For the base:

$$p(q_B(t-1) | Y_B(t-1), \dot{q}_B(t-1), \tau(t-1)) \xrightarrow[\text{dynamics}]{}$$

$$\xrightarrow[\text{dynamics}]{} p(q_B(t) | Y_B(t-1), \dot{q}_B(t-1), \tau(t-1))$$

the predicted probability density is then used with the observation probability to segment the observations Y(t) in $Y_A(t)$, $Y_b(t)$, and $Y_T(t)$ and after to estimate the new values at time t.

$$p(q_B(t) | Y_B(t-1), \dot{q}_B(t-1), \tau(t-1) \xrightarrow[\text{observation}]{}$$

$$\xrightarrow[\text{observation}]{} p(q_B(t) | Y_B(t), \dot{q}_B(t-1), \tau(t-1))$$

Using the Bayes rule and the segmented observation it is possible to determine the a-posteriori density

$$p(q_B(t) | Y_B(t), \dot{q}_B(t-1), \tau(t-1)) =$$

$$k \cdot p(y_B(t) | q_B(t)) \cdot p(q_B(t) | Y_B(t-1), \dot{q}_B(t-1), \tau(t-1))$$

From this expression is possible to compute the new values of joint $\hat{q}_A(t)$, $\hat{q}_B(t)$ and $\hat{q}_T$; these values are sent to Robot and its controlling algorithm computes the joint velocity $\dot{q}_A(t)$, $\dot{q}_B(t)$, $\dot{q}_T(t)$ and the command $\tau(t)$ which are then sent back to main PC for the next estimation at time $t+1$.

Analytic solutions for a-posteriori density are only available for few systems and measurement models, so is necessary to use a stochastic sampling method to find an approximation to probability density [3].

Calling X a random variable with probability density function $f(x) = f_1(x) \cdot f_2(x)$

A set of samples $S := \{s^{(1)}, \ldots, s^{(N)}\}$ with $s^{(n)} \in X$ is drawn randomly from $f_1(x)$. A new samples set S' is built choosing a sample $s^{(k)}$ with probability

$$\pi^{(k)} := \frac{f_2(s^{(k)})}{\sum_{j=1}^{N} f_2(s^{(j)})}$$

From the sample set S. The distribution of S' tends to that of f(x) as $N \to \infty$.

An optimisation procedure has been implemented to refine the estimation of position and attitude of the base. This algorithm performs an object shape restoring, minimising the image plane reproiection error.

2.3 Upgrade of Propulsion System

In its original version, the propulsion system of the vehicle was based upon 8 electron-valves connected to 2 air reservoirs, that provide independent jet thrusts to move and rotate the robot according to three planar degrees of freedom. Convergent nozzles were directly connected to the outflow port of each valve. The navigation control was achieved by firing the thrusters with a simple on-off strategy, governing the variation of the base momentum through the width modulation of the electric pulses that activate the air-jet valves (PWM – Pulse Width Modulation). With this approach, each thruster can provide a fixed linear force of 0.8 N, for a minimum time duration that depends on the net response time of the electron-valve. With such an arrangement, the control of the thrust intensity was not possible, since the electron-valves of the robot are characterised by a fixed outflow section.

A new strategy has been studied for the propulsion system, to make it possible the regulation of the thrust intensity by using again the same electron-valves of the original prototype, obtaining an effect similar to that of a variable-section thruster. In this way, it is possible to achieve a more efficient tracking of the target object, even in case of rapid movements, docking and rendez-vous manoeuvres, without any increase of the system complexity and resources.

The outflow port of each valve has been connected to a Small Reservoir (SR) that acts as an automatic pressure regulator (see figure 2.5)

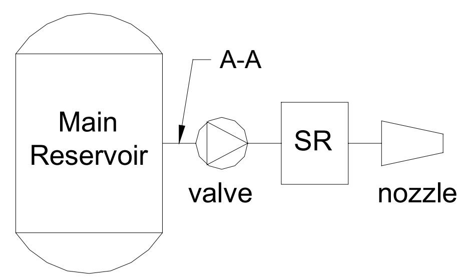

Fig. 2.5 - Schematic of the new arrangement for a thruster.

The air coming from the main reservoir to the Small Reservoir through the valve is continuously exhausted through the nozzle to provide the thrust. A careful design of the pneumatic components (the connection A-A, the SR and the nozzle), together with a PWM control of the valve, can provide a fast adjustment of the air pressure inside the SR and hence the desired thrust regulation. The knowledge of the dynamics of the robot base (e.g. resulting from on-line calculations or measurements) makes it possible to modulate the width of the valve pulses, to achieve a continuous control of the propellant pressure inside the SR. As a result, arbitrary transient thrust profiles can be easily obtained, with low hardware resources and simple control strategies. In this scenario, thanks to new on-board

processing capabilities, the limitation to the pass-band of the thrust-regulation is given by the mechanical properties of the valve (net response time).
Several simulations have been carried out to study the sensitivity of this strategy to the variation of the main system design parameters (geometric constraints of the pneumatic system, required range of regulation for the thrust intensity, etc.) and few possible solutions have been identified to modify the original robot prototype. For example, figure 2.6 shows the possibility of reproducing a sinusoidal thrust profile with the following characteristics:

Mean value: 0.7 N
Amplitude: 0.35 N
Frequency: 20 Hz

The mean error is below 10 % and it is determined by the inertial properties of the valve shaft. A better fitting would be possible with the proposed control strategy, if the net response time of the valve was below 2 ms.

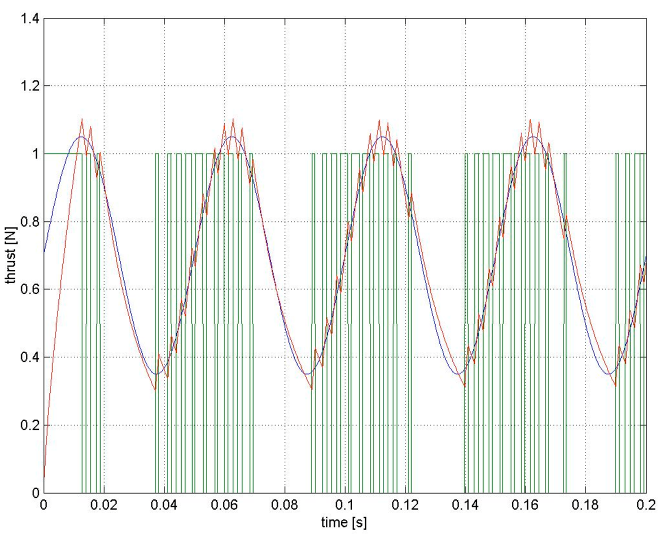

Fig. 2.6 - PWM to control the thrust intensity. Comparison between required and achieved thrust.

3 Robot 3D Extent

Research activity is conducted also on the development of a 3D free flying robot. The purpose of this research effort is to extend 2D robot technologies to a three dimensional testbed simulating conditions of real space operations. The goal is to optimise control strategies to the control of a free flying 3D robot in tracking and capture of a moving object in its working space without thruster firing. During the experiment, the implemented control algorithm should minimise the motion of the robot base compensating the dynamic effect of the arm on it without any thruster action. The innovative aspect of this experiment is that the inertia and mass of the base are of the same order of the arm, resulting in a considerable dynamic coupling and in the need of strong control law in the capture with conventional manipulator control. The effect of the arm deployment during the capture of the target in the three-dimensional space is auto-compensated by the arm motion itself; for this scope redundant degrees of freedom and the condition of non-holonomic motion are used. The challenge is not to use the thrusters to compensate the arm movements, but still obtain a negligible base motion.
The 3D free floating robot is an upgrade of the 2D system which has a 3D workspace. The electronic hardware and software are being upgraded to 3D environment from the existing 2D version.
Space applications concern the use of this kind of robot for space servicing: extra vehicular activity (EVA) or inner vehicular activity. In these applications closing thrusters during the operational time of the robot implies a significative saving of fuel and an increase of the system's useful life.

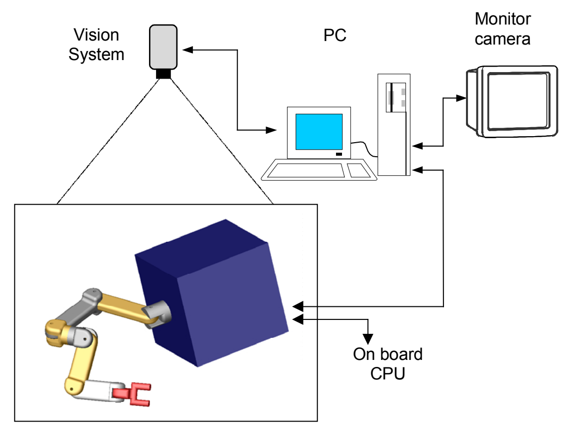

Fig. 3.1– Test bed of the 3D Extent

The project has started with a feasibility study in which it has been verified that the idea of a free floating auto-compensed robot really works. It is foreseen a parabolic fly for testing the functionality of the 3D free flying robot at zero-g.

3.1 Control of the robot base

The 3D prototype is controlled only at the manipulator joints, with no thruster action on the base. This condition leads to the ideal configuration of free-floating system, with internal forces acting and no external forces.

The angular momentum and linear momentum of the multibody system shall remain constant; in particular they will remain zero, if the system was at rest at the beginning of the control action.
In terms of base and manipulator velocities, the resulting equation of the angular momentum links together spacecraft attitude and joint coordinates:

$$\dot{\varphi}_b = [I_{m/b}(\varphi_b, q_m)]\dot{q}_m \qquad (3.1)$$

with the matrix depending on inertia properties of the system.
This expression is already an attitude control law for the base. The desired velocity of the base $\dot{\varphi}_b$ are the input, and with a pseudo-inversion of the matrix the outputs are velocities $\dot{q}_m$ of the arm.
Figure 3.2 shows a 2D simulation of the manoeuvre that takes the base attitude to a desired position, by means of arm motion.

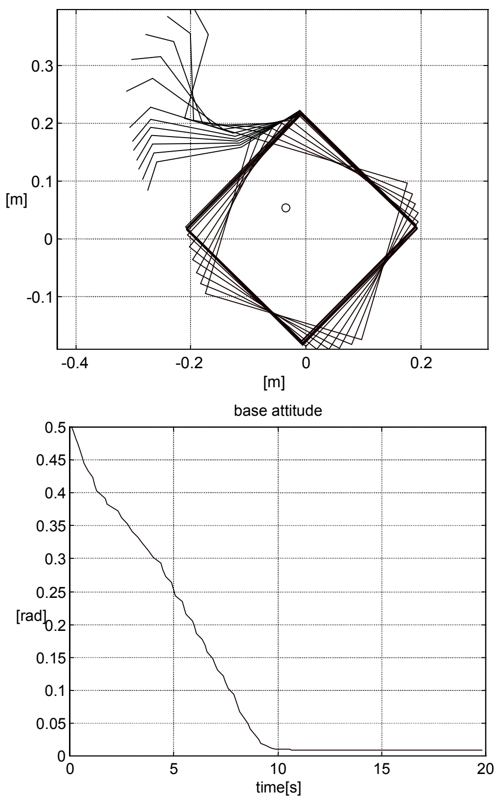

Fig. 3.2 - Simulation of a desired base rotation with arm motion and exploitation of momentum conservation.

3.2 Control of the manipulator end-effector

This multibody cinematic control is well known in free-flyer space robotics literature [4], through the use of *Generalized Jacobian Matrix* (here reported with [J_G] notation), developed by Yoshida and Umetani [5]. The proposed control law compensates the drift of the end-effector (attitude and position) caused by the base motion, during a free-floating manipulation without sensor feedback. In this case, a traditional control law for Fixed base manipulator would fail.
On the other hand, the control with the Generalized Jacobian does not avoid the base motion itself. The latter drift should be avoided or controlled with jet thruster.
Using the Resolved Motion Rate Control (RMRC) or the Torque Control (TC) architectures, the applications of the Generalized Jacobian leads to the following formulations:

$$\dot{q}_m = \left[J_G({}^I\varphi_b, q_m)\right]^{-1}\,{}^I\dot{X}_{EE} \qquad (3.2)$$

$$\Delta q_m = \left[J_G({}^I\varphi_b, q_m)\right]^{T}\,{}^I\Delta X_{EE} \qquad (3.3)$$

Figure 3.3 reports a simulation of the end-effector task.

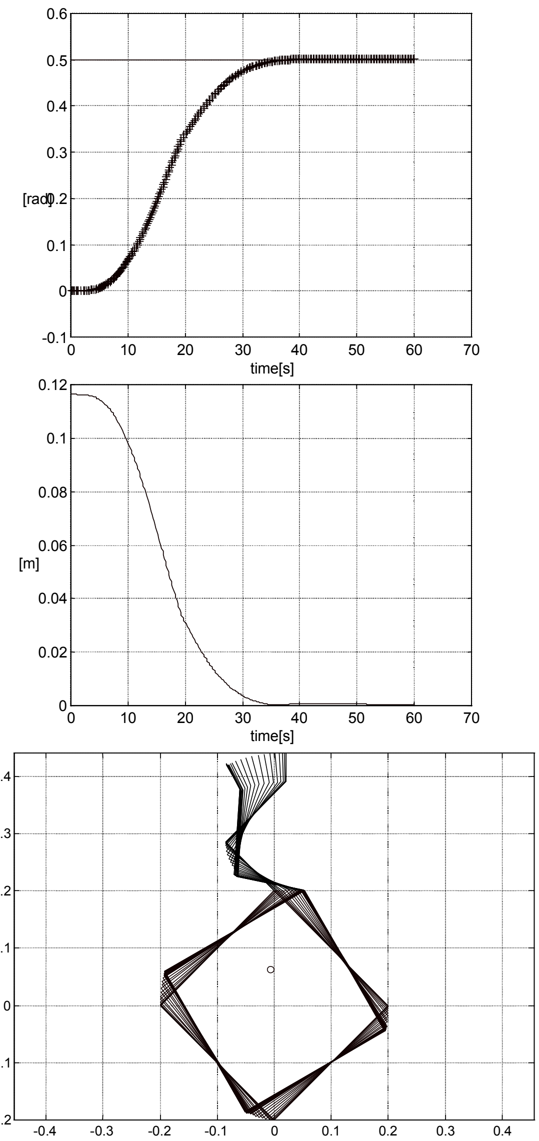

Fig. 3.3 - Simulation of the end-effector task, using the Generalized Jacobian Matrix.

3.4 Coordinated control of the manipulator end-effector and the base attitude

Two different methods are implemented, to obtain the desired coordinated motion of the arm. The aim is to accomplish both end-effector and base attitude tasks.

Combining equation (3.1) with the Generalized Jacobian Matrix (3.2) - reduced for only the end-effector positioning task -, into a two tasks equation for redundancy solution, it is possible to obtain the expression for the coordinated control of end-effector, and base attitude:

$$\dot{q}_m = [JR_G]^+ \dot{X}_{EE} + [I - JR_G{}^+ JR_G][I_{m/b}]^T \dot{\varphi}_b$$

where $[JR_G]$ is the end-effector positioning control matrix - first task -, and the last term is the so called internal motion of the arm to accomplish the control of base rotation - second task. For this method, simulation and stability are reported in [6]

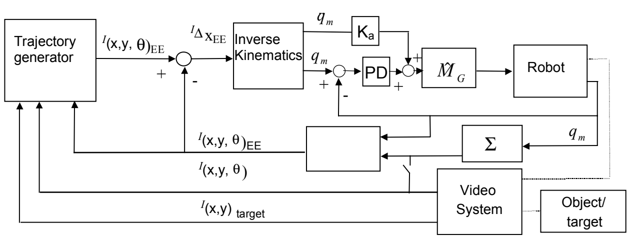

Fig. 3.4 - Control Scheme for manipulation

Another control solution is in the following expression:

$$\dot{q}_m = \begin{bmatrix} [JR_G] \\ [I_{m/b}] \end{bmatrix}^+ \begin{Bmatrix} {}^I\dot{X}_{EE} \\ \dot{\varphi}_b \end{Bmatrix}$$

where the two tasks are resolved at the same time with the linear combination (same matrix form).

This method is sensitive to the number of joint and to their configuration in the joint space. Pseudo-inversion of the matrix can lead to unconditioned or unstable solutions.

4. Conclusions

The presented work focused on the ongoing optimisation activity in free floater and free flyer robotics at Cisas University of Padova. A new test bed has been engineered for 2D simulation of object capture with an improved mechanical and electronic robot architecture, faster control and image elaboration. A new propulsion system has also been designed to allow regulation of the thrust intensity in the navigation phase using on/off electron valves. An optimised control has also been presented to minimise base motion in a thrustless 3D free flyer extent of the 2D robot which is under development for parabolic flight test campaign.

Acknowledgements

This work was partially financed by Italian Space Agency (ASI), within on ground technologies supporting space robotics research.

Reference

[1] M. Marchesi, F. Angrilli, C. Bettanini, “On Ground Experiments of Free-flyer Space Robot Simulator in Intervention Missions”, Proceeding of the 6th International Symposium on Artificial Intelligence and Robotics & Automation in Space: i-SAIRAS 2001, Canadian Space Agency, St-Hubert, Quebec, Canada, June 18-22, 2001.

[2] Carpenter J., Clifford P., Fearnhead P., “Building Robust Simulation-based Filters for Evolving Data Sets”, Internal Report, Department of Statistics, 1, South Parks Road, Oxford, OX1 3TG.

[3] Isard M., Blake A., “Contour tracking by stochastic propagation of conditional density” International Journal of Computer Vision, N° 29, 1, pagg. 5--28, 1998

[4] Y. Xu, T. Kanade, "Space Robotics: Dynamics and Control", Kluwer Academic Publishers, 1993.

[5] K. Yoshida, Y. Umetani, “Resolved Motion Rate Control of Space Manipulator with Generalized Jacobian Matrix”, IEEE Transactions on Robotics and Automation, Vol.5 No.3 June 1989.

[6] B. Siciliano, “Closed-Loop Kinematic Algorithms for Redundant Spacecraft/Manipulator Systems”, IEEE Transactions on Robotics and Automation, 1993.